Advances in Machinery, Materials Science and Engineering Application
M. Chen et al. (Eds.)

doi:10.3233/ATDE220471

Variation Spindle Speed for the Suppression of Chatter in Milling

Chao LI [a,1], Gang ZHENG [a], Sihao MAO [b] and Xu ZHANG [c]
[a] *Shanghai Engineering Research Center of Physical Vapor Deposition (PVD) Superhard Coating and Equipment, Shanghai Institute of Technology, Shanghai, 201418, China*
[b] *School of Mechanical Science & Engineering, Huazhong University of Science and Technology, Wuhan, 430074, China*
[c] *School of Mechatronic Engineering and Automation, Shang University, 200444, China*

Abstract. In metal machining, regenerative chatter seriously affects tool life, part surface quality and cutting efficiency. To suppress chatter generated during milling, researchers have proposed a variable spindle speed technique. But the previous VSS milling model is based on two degrees of freedom system (two-DOF). In this paper, a three-DOF system suitable for VSS milling of thin-walled parts is proposed by introducing the axial contact angle. The improved semi-discretization method is used to solve the dynamical equation and obtain the stability lobe diagram (SLD). Comparing the SLDs under variable speed and constant speed, it shows that the VSS can obtain more stable regions than that of constant spindle speed (CSS). The experimental results show that VSS milling can suppress chatter.

Keywords. Variable spindle speed, milling, chatter, Three-DOF dynamic model

1. Introduction

With increasing demands on processing, the machining requirements of thin-walled components with complex structures are increasing. However, self-excited vibration between tools and workpiece during metal cutting process, which leads to the degradation of quality on part surface and affects tool to machine life. According to the regeneration machine tool chatter proposed by Tobias and Fishwick [1], it is known that the self-excitation vibration caused by the regeneration effect, namely regeneration chatter. To avoid the occurrence of this phenomenon, some methods were proposed. Reducing the depth of cut in machining process achieves the effect of suppressing chatter, but seriously affects machining efficiency. Chatter suppression without compromising machining efficiency, tools with variable pitch [2, 3] or with variable helix angles [4, 5] can be used. Different from the above methods, the spindle variable speed technique can be effectively used for a larger spindle speed range. [6]

In recent years, some researchers have done a lot of theoretical research and experiments on spindle variable speed technology. Sastry et al. [7] proposed the chatter

[1] Chao Li, Corresponding author, Shanghai Engineering Research Center of Physical Vapor Deposition (PVD) Superhard Coating and Equipment, Shanghai Institute of Technology, Shanghai, 201418, China; E-mail: 3468687216@qq.com.

stability analysis of VSS milling based on Floquet theory. Balachandran [8] proposed an improved semi-discrete method for the analysis of VSS up and down milling. Lv [9] proposed a fully-discretized Runge-Kutta method to predict the milling stability of VSS. Zhang et al. [10] proposed the method based on a numerical integration scheme for VSS milling stability prediction. Totis [11] proposed a method to estimate chatter stability at superhigh velocity based on Chebyshev collocation method. Amp [12] that the spindle speed varied in sinusoidal and triangular waveforms, and used the improved semi discrete method to analyze the stability of VSS milling. Brecher [13] used online chatter detection technology and cutting depth to control the spindle speed. Niu [14] proposed a variable step size numerical analysis method based on Floquet theory to predict VSS milling. Jin et al. [15] adopted the improved semi discrete method for stability analysis of variable pitch as well as variable spindle speeds. Previous papers have greatly improved the computational efficiency for predicting chatter stability in VSS milling, but most studies focus on two-DOF milling model. In actual processing, stability analysis of traditional milling system is inaccurate. At present, the three-DOF model analysis is not perfect. In this article, a degree of freedom is added by introducing an axial angle of contact.

The model established in this paper is suitable for complex surfaces and thin-walled parts. The commonly used two-DOF model is not applicable. [16] Therefore, based on the three-DOF model, the use of semi- discretization method is extended in variable speed milling. Compared with two-DOF milling dynamic model, three-DOF milling dynamic model can predict chatter stability more accurately. The second part describes the dynamic equation. The third section describes the stability analysis of VSS milling by using the improved semi-discretization method.

2. Model Milling

When machining complex surfaces and thin-walled parts, the axial chatter between the tool and the workpiece is inevitable, and the traditional end milling model can not meet the requirements. [16] Therefore, the establishment of a three-DOF milling system improves the analysis of chatter stability in VSS milling.

Figure 1 shows the equation of the three-DOF milling system:

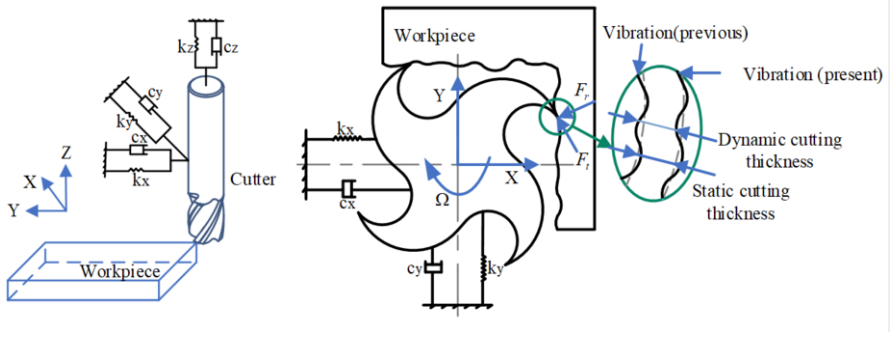

Figure 1. Face-milling system model

$$\begin{pmatrix} m_x & 0 & 0 \\ 0 & m_y & 0 \\ 0 & 0 & m_z \end{pmatrix}\begin{pmatrix} \ddot{x}(t) \\ \ddot{y}(t) \\ \ddot{z}(t) \end{pmatrix}+\begin{pmatrix} 2m_x\xi\omega_n & 0 & 0 \\ 0 & 2m_y\xi\omega_n & 0 \\ 0 & 0 & 2m_z\xi\omega_n \end{pmatrix}\begin{pmatrix} \dot{x}(t) \\ \dot{y}(t) \\ \dot{z}(t) \end{pmatrix}$$
$$+\begin{pmatrix} m_x\omega_n^2 & 0 & 0 \\ 0 & m_y\omega_n^2 & 0 \\ 0 & 0 & m_z\omega_n^2 \end{pmatrix}\begin{pmatrix} x(t) \\ y(t) \\ z(t) \end{pmatrix}=\begin{pmatrix} -K_{xx} & -K_{xy} & -K_{xz} \\ -K_{yx} & -K_{yy} & -K_{yz} \\ -K_{zx} & -K_{zy} & -K_{zz} \end{pmatrix}\begin{pmatrix} x(t) \\ y(t) \\ z(t) \end{pmatrix}+ \tag{1}$$
$$\begin{pmatrix} K_{xx} & K_{xy} & K_{xz} \\ K_{yx} & K_{yy} & K_{yz} \\ K_{zx} & K_{zy} & K_{zz} \end{pmatrix}\begin{pmatrix} x(t-T) \\ y(t-T) \\ z(t-T) \end{pmatrix}$$

where ξ is the relative damping, $m_i(i=x,y,z)$ is the modal mass of the cutter, ω_n is the angular natural frequency. Where $x(t)$, $y(t)$ and $z(t)$ were the vibration and shift of the tools in three directions.

$K_{xx,}$ K_{xy}, K_{xz}, K_{yx}, K_{yy}, K_{yz}, K_{zx}, K_{zx}, K_{zy}, The cutting force coefficient formula is as follows:

$$\begin{cases} K_{xx}=\sum_{j=1}^{N}\sum_{l=1}^{m}\frac{g(\psi_j(t))dz}{\sin\delta}\sin(\psi_j(t))\sin\delta\times(-k_t\cos\psi_j(t)-k_r\sin\psi_j(t)\sin\delta-k_a\sin\psi_j(t)\cos\delta) \\ K_{xy}=\sum_{j=1}^{N}\sum_{l=1}^{m}\frac{g(\psi_j(t))dz}{\sin\delta}\cos(\psi_j(t))\sin\delta\times(-k_t\cos\psi_j(t)-k_r\sin\psi_j(t)\sin\delta-k_a\sin\psi_j(t)\cos\delta) \\ K_{xz}=\sum_{j=1}^{N}\sum_{l=1}^{m}\frac{g(\psi_j(t))dz}{\sin\delta}\cos\delta\times(k_t\cos\psi_j(t)+k_r\sin\psi_j(t)\sin\delta+k_a\sin\psi_j(t)\cos\delta) \\ K_{yx}=\sum_{j=1}^{N}\sum_{l=1}^{m}\frac{g(\psi_j(t))dz}{\sin\delta}\sin\psi_j(t)\sin\delta\times(k_t\cos\psi_j(t)-k_r\cos\psi_j(t)\sin\delta-k_a\cos\psi_j(t)\cos\delta) \\ K_{yy}=\sum_{j=1}^{N}\sum_{l=1}^{m}\frac{g(\psi_j(t))dz}{\sin\delta}\cos\psi_j(t)\sin\delta\times(k_t\sin\psi_j(t)-k_r\cos\psi_j(t)\sin\delta-k_a\cos\psi_j(t)\cos\delta) \end{cases} \tag{2}$$

$$\begin{cases} K_{yz}=\sum_{j=1}^{N}\sum_{l=1}^{m}\frac{g(\psi_j(t))dz}{\sin\delta}\cos\delta\times(-k_t\sin\psi_j(t)+k_r\cos\psi_j(t)\sin\delta+k_a\cos\psi_j(t)\cos\delta) \\ K_{zx}=\sum_{j=1}^{N}\sum_{l=1}^{m}\frac{g(\psi_j(t))dz}{\sin\delta}\sin\psi_j(t)\sin\delta\times(k_r\cos\delta-k_a\sin\delta) \\ K_{zy}=\sum_{j=1}^{N}\sum_{l=1}^{m}\frac{g(\psi_j(t))dz}{\sin\delta}\cos\psi_j(t)\sin\delta\times(k_r\cos\delta-k_a\sin\delta) \\ K_{zz}=\sum_{j=1}^{N}\sum_{l=1}^{m}\frac{g(\psi_j(t))dz}{\sin\delta}\cos\delta\times(-k_r\cos\delta+k_a\sin\delta) \end{cases} \tag{3}$$

where k_a, k_r and k_t are the axial linear and approach linear milling force coefficients, and the tangential linear milling force coefficient, respectively, δ is the axial angle.

The specific position expression of the j-tooth is as follows:

$$\psi_j(t)=\frac{2\pi}{60}\int_0^t\Omega(s)ds+(j-1)\frac{2\pi}{N} \tag{4}$$

where $\Omega(s)$ is a function of speed over time; N indicates the number of teeth;

The function $g(\psi_j(t))$ to determine if the cutter teeth are cutting, the expression is:

$$g(\psi_j(t)) = \begin{cases} 1, & \text{if } \psi_s < \psi_j < \psi_{ex} \\ 0, & otherwise \end{cases} \tag{5}$$

where ψ_{st} and ψ_{ex} represent the starting and leaving angles of jth cutter tooth respectively.

Considering the spindle variable speed of multiple harmonics, the formula of spindle variable speed is:

$$\begin{aligned} \Omega(t) &= \Omega_0 + \Omega_1 \sin(\omega_m t + \varphi) \\ &= \Omega_0 \left[1 + RVA \sin(RVF \frac{2\pi}{60} \Omega_0 t + \varphi) \right] \end{aligned} \tag{6}$$

where Ω_0 is the averge spindle speed. Ω_1 is the amplitude of the speed variation, ω_m is the variation frequency of spindle speed, φ is the phase, and $RVF=60/\Omega_0 T$ is the frequency of the change of the speed of the main shaft. $RVA=\Omega_1/\Omega_0$ is expressed as the ratio of maximum speed to average speed.

Substituting Eq. (6) into Eq. (4), the resulting formula is as follows:

$$\psi_j = \frac{2\pi}{60} \left\{ \Omega_0 t + \frac{60RVA}{2\pi RVF} [1 - \cos(\omega_m t + \varphi)] \right\} + (j-1)\frac{2\pi}{N} \tag{7}$$

The time delay under variable spindle speed can only be obtained by implicit formula:

$$\int_{t-\tau(t)}^{t} \frac{\Omega(s)}{60} ds = \frac{1}{N} \tag{8}$$

Substituting Eq. (6) into Eq. (8), the resulting formula is as follows:

$$\frac{1}{60} \left(\Omega_0 \tau(t) + \frac{\Omega_1}{\omega_m} \cos\left(\omega_m \left(t - \tau(t) \right) + \varphi \right) - \frac{\Omega_1}{\omega_m} \cos(\omega_m t + \varphi) \right) = \frac{1}{N} \tag{9}$$

In general, $\tau(t)$ cannot be solved, and when taking the RVF and RVA to be approximately "infinitesimal", the expression of $\tau(t)$ is:

$$\begin{aligned} \tau(t) &\approx \tau_0 - \tau_1 \sin(\omega_m t + \varphi) \\ &= \tau_0 \left[1 - RVA \cdot \sin\left(RVF \cdot \frac{2\pi}{60} \Omega_0 t \right) \right] \end{aligned} \tag{10}$$

where $\tau=60/N\Omega_0$ and $\tau_1/\tau_0=\Omega_1/\Omega_0$.

3. Chatter Stability Analysis Based on VSS Milling

The three-DOF milling dynamics equation can be transformed into an n-dimensional linear delay differential equation considering the regeneration effect:

$$\dot{\gamma}(t) = C_0\gamma(t) + C(t)\gamma(t) - C(t)\gamma(t-\tau(t)) \tag{11}$$

Where $\boldsymbol{C_0}$ is the matrix of time-invariant coefficients, and $\boldsymbol{C(t)}$ is a matrix of periodic coefficients satisfying $\boldsymbol{C(t)=C(t+\tau(t))}$, Taking the average delay τ_0 into ρ a interval Δt, that is $\tau_0=\rho\Delta t$. For Eq. (1), and the initial conditions under which Eq $\gamma(t_i)=\gamma_i$, the differential equations are further optimized during the period $[t_i,t_{i+1}]$:

$$\gamma(t) = e^{C_0(t-t_i)}\gamma_i + \int_{t_i}^{t}\left\{e^{C_0(t-\theta)}C(\theta)\left[\gamma(\theta)-\gamma(\theta-\tau_i)\right]\right\}d\theta \tag{12}$$

For Eq. (2), this is the same thing:

$$\gamma_{i+1} = \gamma(t_i+\Delta t) = e^{C_0(\Delta t)}\gamma_i + \int_{t_i}^{t_i+\Delta t}\left\{e^{C_0(t+\Delta t-\theta)}C(\theta)\left[\gamma(\theta)-\gamma(\theta-\tau_i)\right]\right\}d\theta \tag{13}$$

The expression for the time-lapse τ_i of the discrete interval is:

$$\tau_i = \frac{1}{\Delta t}\int_{t_i}^{t_i+\Delta t}\tau(t)dt \tag{14}$$

$C(t)$, $\gamma(t)$, $\gamma(t\text{-}\tau(t))$ approximate to:

$$C(t) = C_i + \frac{C_{i+1}-C_i}{\Delta t}(t-t_i) \tag{15}$$

$$\gamma(t) = \gamma_i + \frac{\gamma_{i+1}-\gamma_i}{\Delta t}(t-t_i) \tag{16}$$

$$\gamma(t-\tau_i) = \beta_i\gamma_{i-M} + \alpha_i\gamma_{i-M+1} \tag{17}$$

The approximate weights α_i, β_i, and the expression for the delay time length of M is:

$$\alpha_i = \frac{\tau_i + \Delta t/2 - m_i\Delta t}{\Delta t} = \frac{\tau_i}{\Delta t} + \frac{1}{2} - m_i \tag{18}$$

$$\beta_i = \frac{-\tau_i + \Delta t/2 + m_i \Delta t}{\Delta t} = -\frac{\tau_i}{\Delta t} + \frac{1}{2} + m_i \tag{19}$$

$$M = \max\left\{m_i\right\} = \max\left\{\text{int}\left(\frac{\tau_i}{\Delta t} + 0.5\right)\right\} \tag{20}$$

Substituting the above three formulas into Eq. (3):

$$\gamma_{i+1} = (\upsilon_0 + \eta_i)\gamma_i + R_i\gamma_i + \beta Q_i \gamma_{i-M} + \alpha_i Q_i \gamma_{i-M+1} \tag{21}$$

$$\begin{cases} \eta_i = \left(\upsilon_1 - \dfrac{2}{\Delta t}\upsilon_2 + \dfrac{1}{\Delta t^2}\upsilon_3\right)C_i + \left(\dfrac{1}{\Delta t}\upsilon_2 - \dfrac{1}{\Delta t^2}\upsilon_3\right)C_i \\ R_i = \left(\dfrac{1}{\Delta t}\upsilon_2 - \dfrac{1}{\Delta t^2}\upsilon_3\right)C_i + \left(\dfrac{1}{\Delta t^2}\upsilon_3\right)C_{i+1} \\ Q_i = \left(\upsilon_1 - \dfrac{1}{\Delta t}\upsilon_2\right)C_i + \left(\dfrac{1}{\Delta t}\upsilon_2\right)C_{i+1} \end{cases} \tag{22}$$

$$\begin{cases} \upsilon_0 = e^{C_0' \Delta t} \\ \upsilon_1 = C_0^{-1}(\upsilon_0 - I) \\ \upsilon_2 = C_0^{-1}(\upsilon_i - \Delta t I) \\ \upsilon_3 = C_0^{-1}(2\upsilon_0 - \Delta t^2 I) \end{cases} \tag{23}$$

where ***I*** stands for unit matrix.

The expression for the diastolic dispersion is:

$$G_{i+1} = D_i G_i \tag{24}$$

Where:

$$G_{i+1} = col\left(\gamma_i, \gamma_{i-1} \cdots \gamma_{i-M}\right) \tag{25}$$

$$D_i = \begin{pmatrix} \left(I - R_i\right)^{-1}\left(\upsilon_0 + \eta_i\right) & 0 & \cdots & 0 & \left(I - R_i\right)^{-1}\alpha_i Q_i & \left(I - R_i\right)^{-1}\beta_i Q_i \\ I & 0 & \cdots & 0 & 0 & 0 \\ 0 & I & \cdots & 0 & 0 & 0 \\ \vdots & \vdots & \cdots & \vdots & \vdots & \vdots \\ 0 & 0 & \cdots & 0 & I & 0 \end{pmatrix} \tag{26}$$

The Floquet transmission array is $\boldsymbol{D=D_{k-1}D_{k-2}\cdots D_0}$. Derived from Floquet theory, whether it is stable in the milling process can be determined by eigenvalues. [1,5] It is determined according to whether the characteristic value is greater than 1. When less than 1, the system is stable, and vice versa.

Then, set $\gamma=\begin{bmatrix}q(t) & p(t)\end{bmatrix}^T$, $q(t)=\begin{Bmatrix}x(t)\\y(t)\\z(t)\end{Bmatrix}$, $p(t)=\begin{Bmatrix}m_x\dot{x}(t)+m_x\varsigma\omega_n x(t)\\m_y\dot{y}(t)+m_y\varsigma\omega_n y(t)\\m_z\dot{z}(t)+m_z\varsigma\omega_n z(t)\end{Bmatrix}$. Finally, the final three-DOF milling model can be expressed as:

$$\dot{\gamma}(t)=C_0\gamma(t)+C(t)\gamma(t)-C(t)\gamma(t-\tau(t)) \tag{27}$$

Where:

$$C_0=\begin{pmatrix}-\varsigma\omega_m & 0 & 0 & \frac{1}{m_x} & 0 & 0\\ 0 & -\varsigma\omega_m & 0 & 0 & \frac{1}{m_y} & 0\\ 0 & 0 & -\varsigma\omega_m & 0 & 0 & \frac{1}{m_z}\\ m\omega_n^2(\varsigma^2-1) & 0 & 0 & -\varsigma\omega_m & 0 & 0\\ 0 & m\omega_n^2(\varsigma^2-1) & 0 & 0 & -\varsigma\omega_m & 0\\ 0 & 0 & m\omega_n^2(\varsigma^2-1) & 0 & 0 & -\varsigma\omega_m\end{pmatrix} \tag{28}$$

$$C(t)=\begin{pmatrix}0 & 0 & 0 & 0 & 0 & 0\\ 0 & 0 & 0 & 0 & 0 & 0\\ 0 & 0 & 0 & 0 & 0 & 0\\ K_{xx} & K_{xy} & K_{xz} & 0 & 0 & 0\\ K_{yx} & K_{yy} & K_{yz} & 0 & 0 & 0\\ K_{zx} & K_{zy} & K_{zz} & 0 & 0 & 0\end{pmatrix} \tag{29}$$

The expression of time step ρ is:

$$\Delta t=\frac{\tau_0}{\rho}=\frac{2\pi}{\rho\omega_m}=\frac{60}{\rho\cdot RVF\cdot\Omega_0} \tag{30}$$

The integer m_i is obtained from Eq. (3):

$$m_i=\operatorname{int}\left(\frac{\tau_i+\Delta t/2}{\Delta t}\right)=\operatorname{int}\left(\frac{\rho RVF(1-RVAc_i)}{N}+0.5\right) \tag{31}$$

Where:

$$c_i = \frac{\rho}{\pi}\int_{i\cdot 2\pi/k}^{(i+1)\cdot 2\pi/k} \sin(t)dt, i = 0,1,...,\rho-1 \tag{32}$$

4. Dynamics in Milling Process with VSS

To verify the algorithm in this paper, select Gu's paper for the modal parameters. [16] The number of teeth of the milling system is 4, the modal mass is 0.03993, and the natural frequency is 922Hz. The relative damping ξ=0.011, and the cutting force coefficient kt=1562.1Mpa, ka=538.6Mpa, kr=563.2Mpa.

Based on the comprehensive research status, the chatter situation of the analytical tool is selected to analyze, so the stiffness of the workpiece is assumed to be much larger than that of the tool and the flexibility of the workpiece is ignored. A model for a three-DOF based on VSS milling solved by a modified semi discretization method. The stability lobe diagram of spindle with change speed is compared with that of spindle with constant speed. In Figure 1, the milling stability lobe diagram with a 10% immersion rate is obtained, taking spindle speed and axial cutting depth as horizontal and vertical coordinates. Seguy et al. [17] considered the acceleration of the machine tool spindle and the rated range of spindle speed. Therefore, RVA ≤ 0.3. RVF ≠1, Otherwise, the spindle has only one replacement cycle during one rotation of the tool.

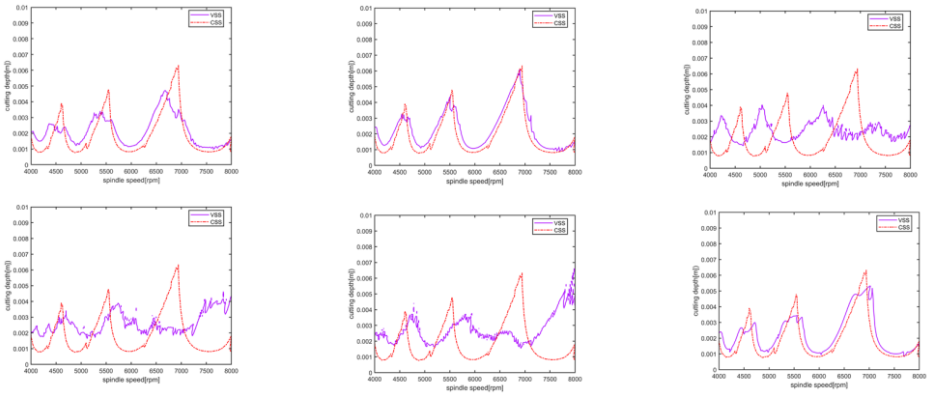

Figure 1. Stability prediction for 10% immersion: (a) RVA=0.2, RVF=0.1, φ=0rad (b) RVA=0.2, RVF=0.1, φ=0.1667rad (c) RVA=0.1, RVF=0.1, φ=0.1667 rad (d)RVA=0.05, RVF=0.5, φ=0rad (e) RVA=0.05, RVF=0.5, φ=0.6667rad (f) RVA=0.05, RVF=0.1, φ=0.6667rad.

For *RVA* = 0.2, 0.1 and *RVF* = 0.1 (see figures 2a-c), the stable region obtained by VSS milling at 4000rpm to 8000rpm is significantly larger than that obtained by CSS milling. For *RVA*=0.05 and *RVF*=0.5, 0.1 (see figures 2d-f), the stability lobe map obtained by VSS milling is close to that obtained by CSS milling. Figure 2 shows that the RVA parameter plays a large role in VSS milling and *RVF* plays a minor role.

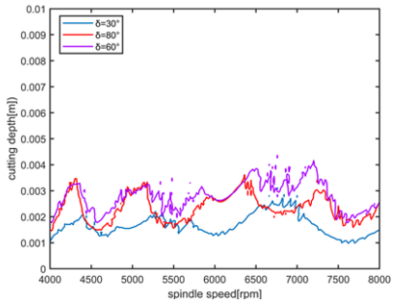

Figure 3. The stability lobe diagram at different axial contact angle: *RVA=0.1, RVF=0.1*.

Figure 3 shows the stability lobes obtained at different axial contact angles. The stability range is the smallest when the discretization angle is 30 degrees. The speed range of the main shaft was from 6500rpm to 7500rpm, and the stable region is obtained when the axial contact angle is 60 degrees and the stable region is larger than 80 degrees.

5. Conclusions

In this paper, the improved semi discrete method is used to predict the VSS milling of three-DOF system. Taking the three-DOF dynamic milling system as the research object, the influence of spindle speed on the stability of the system is studied. The results show that in some spindle speed ranges, the stable region obtained by VSS milling is greater than that obtained by CSS milling. In addition, more stable areas can be obtained by selecting the appropriate axial contact angle in machining.

References

[1] Tobias SA and Fishwick W. Theory of regenerative machine tool chatter. The Engineer. 1958; 250(7): 199-203.
[2] Budak E. An analytical design method for milling cutters with nonconstant pitch to increase stability, Part 2: Application. Journal of Manufacturing Science and Engineering. 2003; 125(1).
[3] Altintas Y, Engin S and Budak E. Analytical stability prediction and design of variable pitch cutters. Journal of Manufacturing Science & Engineering. 1999; 121(2): 173-178.
[4] Sims ND, Mann B and Huyanan S. Analytical prediction of chatter stability for variable pitch and variable helix milling tools. Journal of Sound & Vibration. 2008; 317(3–5): 664-686.
[5] Stone BJ. The effect of the chatter behaviour of machine tools of cutters with different helix angles on adjacent teeth. 1970.
[6] Takemura T, Kitamura T and Hoshi T. Active suppression of chatter by programed variation of spindle speed. Journal of the Japan Society of Precision Engineering. 1975; 41(484): 489-494.
[7] Sastry, et al. Floquet theory based approach for stability analysis of the variable speed face-milling process. Journal of Manufacturing Science & Engineering. 2002.
[8] Long XH and Balachandran B. Stability of up-milling and down-milling operations with variable spindle speed. Journal of Vibration & Control. 2017.
[9] Lv S and Zhao Y. Stability of milling process with variable spindle speed using runge–kutta-based complete method. Mathematical Problems in Engineering. 2021.
[10] Zhang C, Yan Z and Jiang X. Numerical integration scheme–based semi-discretization methods for stability prediction in milling. The International Journal of Advanced Manufacturing Technology. 2021; (4).

[11] Totis G, et al. Efficient evaluation of process stability in milling with Spindle Speed Variation by using the Chebyshev Collocation Method. Journal of Sound & Vibration. 2014; 333(3): 646-668.
[12] Amp SBS and PeignÃ GG. Suppression of period doubling chatter in high-speed milling by spindle speed variation. Machining Science & Technology. 2011; 15(2): 153-171.
[13] Brecher C, Chavan P and Epple A. Efficient determination of stability lobe diagrams by in-process varying of spindle speed and cutting depth. Advances in Manufacturing. 2018; 6(3): 8.
[14] Niu J, et al. Stability analysis of milling processes with periodic spindle speed variation via the variable-step numerical integration method. Journal of Manufacturing Science & Engineering. 2016.
[15] Jin G, et al. Stability analysis of milling process with variable spindle speed and pitch angle considering helix angle and process phase difference. Mathematical Problems in Engineering. 2021; 2021(2): 1-15.
[16] Gu D, et al. Three degrees of freedom chatter stability prediction in the milling process. Journal of Mechanical Science and Technology. 2020; 34(9): 3489-3496.
[17] Seguy S, et al. Control of chatter by spindle speed variation in high-speed milling. Advanced Materials Research. 2010; 112: 179-186.